Acta Biochim Biophys Sin 2014, 46: 40–47 | © The Author 2013. Published by ABBS Editorial Office in association with Oxford University Press on behalf of the Institute of Biochemistry and Cell Biology, Shanghai Institutes for Biological Sciences, Chinese Academy of Sciences. DOI: 10.1093/abbs/gmt126.
Advance Access Publication 1 December 2013

Original Article

Prostaglandin E_2 modulates F-actin stress fiber in FSS-stimulated MC3T3-E1 cells in a PKA-dependent manner

Xiaoyuan Gong[1,2], Weidong Yang[3], Liyun Wang[3], Randall L. Duncan[3]*, and Jun Pan[1]*

[1]Key Laboratory for Biorheological Science and Technology of Ministry of Education, College of Bioengineering, Chongqing University, Chongqing 400044, China
[2]Center for Joint Surgery, Southwest Hospital, The Third Military Medical University, Chongqing 400038, China
[3]Departments of Mechanical Engineering and Biological Sciences, University of Delaware, Newark, DE 19716, USA
*Correspondence address. Tel: +86-23-65460031; Fax: +86-23-65460031, panj@cqu.edu.cn (J.P.); Tel: +1-302-831-4296; Fax: +1-302-8312281; rlduncan@udel.edu (D.L.R)

The effect of prostaglandin E_2 (PGE_2) on bone mass has been well-established *in vivo*. Previous studies have showed that PGE_2 increases differentiation, proliferation, and regulates cell morphology through F-actin stress fiber in statically cultured osteoblasts. However, the effect of PGE_2 on osteoblasts in the presence of fluid shear stress (FSS), which could better uncover the anabolic effect of PGE_2 *in vivo*, has yet to be examined. Here, we hypothesized that PGE_2 modulates F-actin stress fiber in FSS-stimulated MC3T3-E1 osteoblastic cells through protein kinase A (PKA) pathway. Furthermore, this PGE_2-induced F-actin remodeling was associated with the recovery of cellular mechanosensitivity. Our data showed that treatment with 10 nM $dmPGE_2$ for 15 min significantly suppressed the F-actin stress fiber intensity in FSS-stimulated cells in a PKA-dependent manner. In addition, $dmPGE_2$ treatment enhanced the cells' calcium peak magnitude and the percentage of responding cells in the second FSS stimulation, though these effects were abolished and attenuated by co-treatment with phalloidin. Our results demonstrated that 10 nM $dmPGE_2$ was able to accelerate the 'reset' process of F-actin stress fiber to its pre-stimulated level partially through PKA pathway, and thus promoted the recovery of cellular mechanosensitivity. Our finding provided a novel cellular mechanism by which PGE_2 increased bone formation as shown *in vivo*, suggesting that PGE_2 could be a potential target for treatments of bone formation-related diseases.

Keywords prostaglandin E_2; intracellular calcium; cytoskeleton; PKA pathway; fluid shear stress (FSS)

Received: August 9, 2013 Accepted: September 30, 2013

Introduction

Prostaglandin E_2 (PGE_2), a 20-carbon proinflammatory prostanoid, has various physiological effects on tissue. In particular, the anabolic effect of PGE_2 on bone has been established *in vivo* [1,2]. *In vitro* studies have showed that PGE_2 stimulates differentiation by elevating the intracellular cAMP level at low concentrations ($\sim 10^{-8}$–10^{-7} M), while stimulates proliferation through phosphatidyl inositol turning over at high concentrations ($\sim 10^{-6}$–10^{-5} M) in statically cultured MC3T3-E1 osteoblastic cells [3–6]. However, during daily activities, bone cells are constantly stimulated by mechanical force, and the presence of mechanical force alters the release of biochemical factors [7,8] and the involvements of signaling pathways [9,10]. Thus, the cellular effect of PGE_2 in the presence of mechanical loading could be different from that in the static condition, which worth to be studied.

It is well accepted that mechanical loading in bone is anabolic in tissue and at cellular levels. Fluid shear stress (FSS), as one kind of common mechanical stimulation in bone [11], deformed the cell body, thus introducing rapid increase in intracellular calcium concentration ($[Ca^{2+}]_i$) [12] and the release of adenosine triphosphate (ATP) and PGE_2 [8] in osteoblasts. However, the mechanosensitivity of osteoblasts was found to be decreased during continuous FSS stimulation, but recovered after inserting a rest period [13]. The cytoskeleton, a mechanotransductor during FSS stimulation, was believed to play a central role in the regulation of cellular mechanosensitivity through the modulation of mechanosensitive calcium channel (MSCC) activity [14,15]. While PGE_2 has been shown to be capable of affecting cell morphology through modulating F-actin stress fiber in statically cultured osteoblasts [16] and also capable of promoting osteogenic differentiation in rat tendon stem cells [17], the PGE2-regulated F-actin stress fiber remodeling in the presence of mechanical stimulation and its effect on cellular mechanosensitivity have yet to be addressed.

Protein kinase A (PKA) pathway is involved in mechanosensitivity regulation in bone cells. Activation of PKA has been shown to enhance the intracellular calcium response

Downloaded from https://academic.oup.com/abbs/article/46/1/40/1399 by guest on 10 April 2024

during FSS stimulation [18] and is involved in both FSS-induced ERK activation [19] and cyclooxygenase-2 up-regulation [20]. Furthermore, PKA-regulated RhoA GTPase suppression has also been demonstrated previously [21], suggesting that PKA is capable of modulating F-actin stress fiber [14,18]. Moreover, PGE_2 triggers intracellular cAMP elevation in MC3T3-E1 osteoblastic cells at low concentrations [3]. These data suggested that there was a connection between PKA and PGE_2-regulated F-actin remodeling in osteoblasts.

In this study, we hypothesized that PGE_2 modulated F-actin stress fiber in FSS-stimulated MC3T3-E1 osteoblastic cells through PKA pathway and that this PGE_2-induced F-actin remodeling was associated with the recovery of cellular mechanosensitivity. To test this hypothesis, cells were treated with $dmPGE_2$ post FSS stimulation; the involvement of PKA pathways on F-actin modulation was investigated by using 8-Br-cAMP/PKI. To test the effect of $dmPGE_2$-induced F-actin stress fiber remodeling on the recovery of cellular mechanosensitivity, cells were treated with vehicle, $dmPGE_2$, and $dmPGE_2$ plus phalloidin between two bouts of FSS stimulations. The FSS-induced $[Ca^{2+}]_i$ transient was used as an indicator of cellular mechanosensitivity.

Materials and Methods

Materials

16,16-Dimethyl prostaglandin-E_2 ($dmPGE_2$; Cayman, Ann Arbor, USA) was used in this study due to its prolonged half life and bioactivities similar to PGE_2 [22]. Based on the finding that PGE_2 inhibits DNA synthesis by stimulating differentiation at low concentrations ($\sim 10^{-8}$–10^{-7} M) in MC3T3-E1 cells [3,4], $dmPGE_2$ was used at a final concentration of 10 nM. Phalloidin (Sigma, St Louis, USA), an actin stabilizer, was used at a final concentration of 1 μM. 8-Bromoadenosine 3′, 5′-cyclic monophosphate sodium salt (8-Br-cAMP, Sigma), an agonist of PKA pathway, was dissolved in distilled water at a stock concentration of 15 mg/ml and used at a final concentration of 100 μM. The cAMP-dependent protein kinase peptide inhibitor (PKI; Promega, Madison, USA), an inhibitor of PKA pathway, was used at a final concentration of 10 μM. All the final solutions were prepared with the flow medium that was used in F-actin staining and calcium imaging studies. The concentration of agonist or inhibitor was chosen based on our previous studies [14,23].

Cell culture

MC3T3-E1 cells were purchased from American Type Culture Collection (ATCC; Manassas, USA). Cells were grown in α-MEM (Sigma) containing 10% fetal bovine serum (FBS; Gibco, Carlsbad, USA) and 1% penicillin G and streptomycin (Sigma) and maintained in a humidified incubator at 37°C with 5% CO_2. Cells were seeded onto type-I collagen coated glass slides at an initial density of 4×10^4 cells/cm^2 and used for calcium imaging and cytoskeleton staining studies once reaching 80% of confluence. Cells were serum starved overnight prior to each experiment. Cells of 3–10 passages were used in our study.

F-actin staning

The slide containing MC3T3-E1 cells was mounted to a custom designed parallel plate flow chamber [24] and subject to 20 min of FSS at 12 dyn/cm^2 by using aerated (5% CO_2/95% air) flow medium (α-MEM supplemented with 0.1% FBS, v/v) in a cell incubator (37°C). After FSS loading, cells were treated with $dmPGE_2$, $dmPGE_2$ plus phalloidin, $dmPGE_2$ plus PKI, 8-Br-cAMP, 8-Br-cAMP plus PKI, and vehicle (α-MEM supplemented with 0.1% FBS, v/v) for 15 min, respectively (**Fig. 1A**). After all treatments, cells were immediately washed with ice cold phosphate buffered saline (PBS), fixed with 2% paraformaldehyde and 0.1% triton X-100, and stained with Alexa Fluor 488 phalloidin (1 : 40 dilution; Invitrogen, Grand Island, USA) and DRAQ5™ (1 : 2000 dilution; Biostatus Ltd., Leicestershire, UK). Stained cells were imaged on an inverted confocal laser scanning microscope (Zesis LSM 510; Heidenheim, Germany) using 488 and 631 nm excitations with a 40× objective. Since the F-actins network is a 3D structure, to minimize the variation among different batches, we thus recorded our images by focusing the z-level of most nucleuses in a random view. Each experiment was repeated thrice and at least 9 image fields of 40× magnitude were obtained in each trial.

Image quantification

Volocity software (version4.3; Improvision, Waltham, USA) was used to process the areal fraction of continuous F-actin stress fibers in individual cells from well-documented confocal images (**Supplementary Fig. S1**). To account for the variations of staining process and laser intensity, which were unavoidably present among different batches of tests, we obtained a correction factor based on the nuclei staining intensity, since the nucleus was supposed to have a relatively constant intensity. This correction factor was used to linearly adjust the actin staining in each image. The continuous F-actin stress fibers were identified by setting two thresholds: objective intensity larger than 60, and an objective size larger than 500 pixels. The total area was obtained by setting a much lower threshold (larger than 7) and using the 'fill holes in objects' option. The areal fraction of the continuous F-actin stress fibers was calculated, with the total areal of continuous F-actin stress fibers being divided by the total area of cell. For each experimental group, three slides and 16–36 cells were processed.

Downloaded from https://academic.oup.com/abbs/article/46/1/40/1399 by guest on 10 April 2024

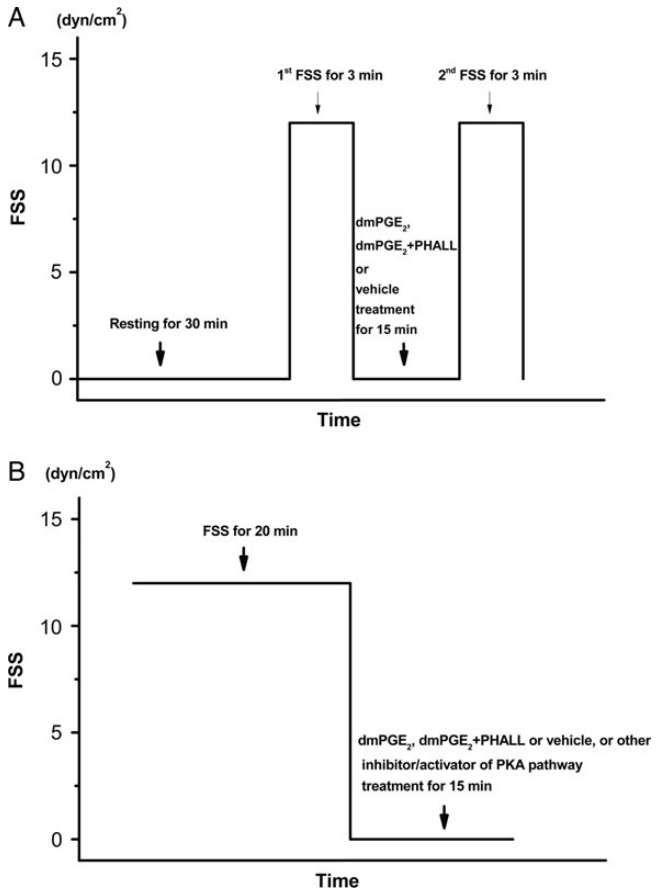

Figure 1. Experimental designs (A) The time course of F-actin staining. MC3T3-E1 cells were subject to FSS stimulation (12 dyn/cm^2) for 20 min, then treated with $dmPGE_2$ (10 nM), $dmPGE_2$ (10 nM) + phalloidin (Phall, 1 μM), vehicle, $dmPGE_2$ (10 nM) + PKA inhibitor (PKI, 10 μM), PKA activator (8-Br-cAMP, 100 μM), and PKI (10 μM) + 8-Br-cAMP (100 μM) for 15 min in static. F-actin was immediately stained after all treatments. (B) The time course of intracellular calcium imaging. MC3T3-E1 cells were subjected to two bouts of FSS stimulation (3 min at 12 dyn/cm^2), between which cells were treated with $dmPGE_2$ (10 nM), $dmPGE_2$ (10 nM) + phalloidin (PHALL, 1 μM) or vehicle for 15 min in static. The intracellular calcium response was recorded during the two FSS loading processes.

Calcium imaging

Cells were washed with PBS, stained with 12 μg/ml Fluo-4 AM (Invitrogen) in α-MEM for 45 min at 37°C, and then washed with PBS again to remove the dye. The slide was mounted to a custom-designed parallel plate flow chamber [24], and fixed to the stage of a fluorescent microscope (Leica Microsystems, Wetzlar, Germany). Flow medium (α-MEM supplemented with 2% FBS, v/v), preserved at 37°C, was slowly driven into the chamber by a peristaltic pump (Longer Peristaltic Pump). The higher concentration of FBS (2%) in calcium imaging than that in F-actin staining study (0.1%) was used to ensure attachment and growth of MC3T3-E1 during the whole experimental process. After resting for 30 min, dynamic fluorescence intensity inside a randomly selected field (1431 × 1059 μm in dimensions) was recorded by real-time $[Ca^{2+}]_i$ imaging with a 20× objective at room temperature. The recording time course included a 60-s baseline, followed by two sequential FSS sessions (3 min each at 12 dyn/cm^2) with a 15 min rest period inserted in between, during which $dmPGE_2$, $dmPGE_2$ plus phalloidin or vehicle (α-MEM supplemented with 2%FBS, v/v) was added to flow medium to test the effect of $dmPGE_2$ on the calcium response recovery and the involvement of F-actin intensity in second FSS (**Fig. 1B**). Image J (version 1.44p, http://rsb.info.nih.gov/ij/) was used to analyze the fluorescence intensity in individual cells, which was normalized with the mean background intensity obtained in three randomly chosen blank areas. The calcium peak magnitude was reported as the fold increment of the peak intensity over the mean baseline fluorescence intensity (=1). The percentage of responding cells was determined for each test (the number of cells whose calcium peak magnitude was over 1.25 fold of baseline was divided by the number of total cells). The 1.25-fold baseline threshold was chosen based on our previous study [12] using Fluo-2 under 12 dyn/cm^2, in which MC3T3-E1 cells remained the same, with regard to the ability of reacting with FSS (percentage of responding cells). Each experiment was repeated thrice and 47–102 cells per group were processed.

Statistical analysis

Data were presented as mean ± SD. For the cytoskeleton image quantification data, statistical significance was determined by using one way analysis of variance (ANOVA) with Bonferroni's *post hoc* test. A P value of <0.05 indicated statistical significance in all analyses. For calcium imaging data, the statistical significance of the calcium peak magnitude and the percentage of responding cells in all treatments were determined by a one-way ANOVA with Bonferroni's *post hoc* test and χ^2 test, respectively.

Results

Effects of $dmPGE_2$ and PKA pathway on F-actin intensity

When compared with FSS plus vehicle treatment group (**Fig. 2A**, b), $dmPGE_2$ treatment after FSS stimulation significantly decreased the FSS-induced F-actin stress fiber intensity (**Fig. 2A**, c) to nearly pre-FSS status (**Fig. 2A**, a). Co-treated cells with $dmPGE_2$ plus phalloidin (**Fig. 2A**, d) or $dmPGE_2$ plus PKI (**Fig. 2C**, a) caused an impaired inhibitory effect of $dmPGE_2$. Similar to $dmPGE_2$ post treatment, 8-Br-cAMP suppressed the F-actin stress fiber intensity in FSS-stimulated cells (**Fig. 2C**, b), which was again abolished by co-treatment with PKI (**Fig. 2C**, c).

Downloaded from https://academic.oup.com/abbs/article/46/1/40/1399 by guest on 10 April 2024

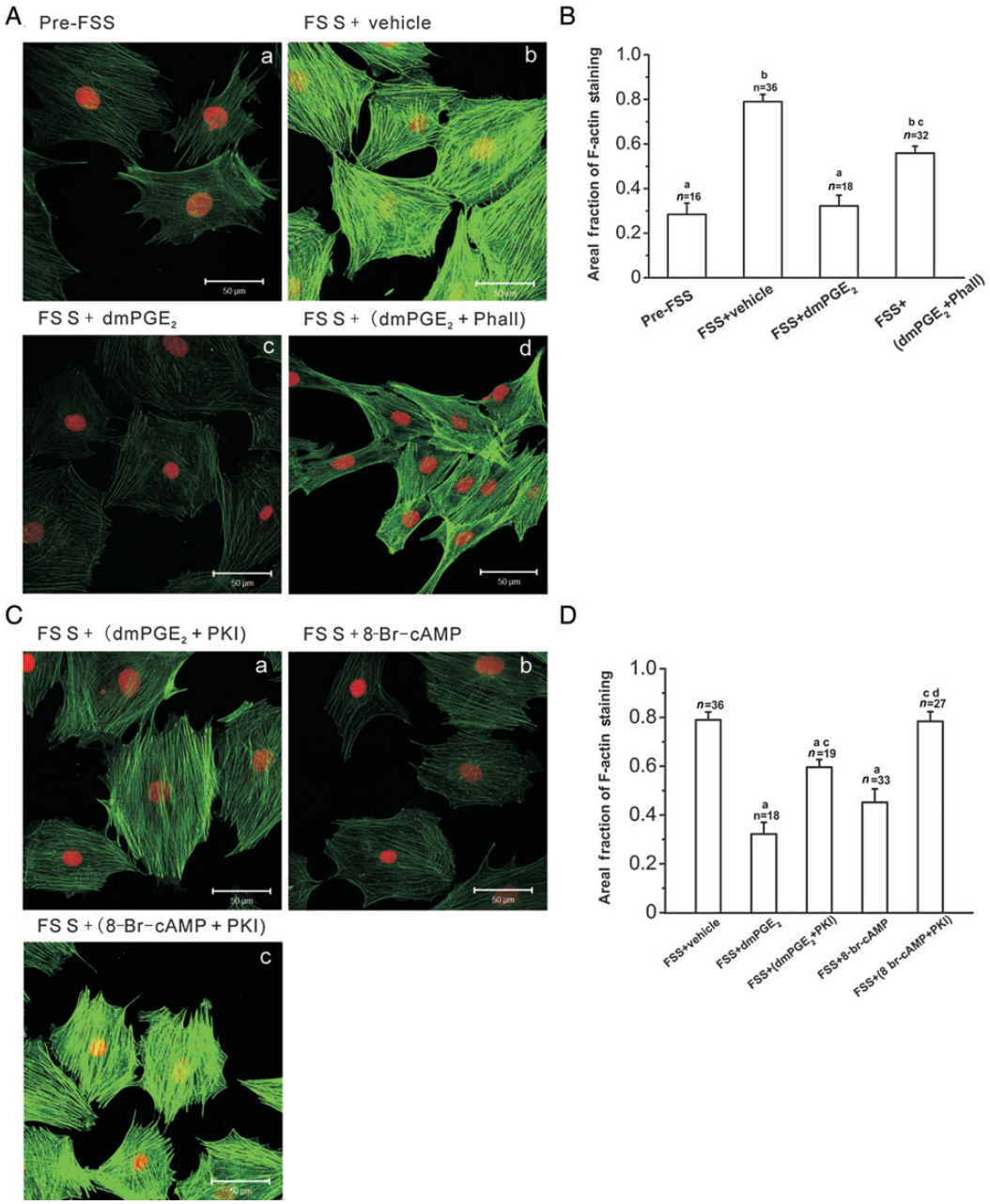

Figure 2. Involvement of PKA in $dmPGE_2$-modulated F-actin remodeling (A) Representative F-actin and nuclei staining showing effect of $dmPGE_2$ on F-actin stress fiber intensity in MC3T3-E1 cells (a–d). (B) Quantification results of (A). Compared with Pre-FSS, FSS + vehicle treatment significantly increased the F-actin stress fiber intensity, which was greatly decreased by FSS + $dmPGE_2$. Phalloidin (Phall) significantly attenuated the effect of $dmPGE_2$. (C) Representative F-actin and nuclei staining showing the involvement of PKA in $dmPGE_2$-modulated F-actin stress fiber intensity (a–c). (D) Quantification results of (C). The effect of $dmPGE_2$ was significantly attenuated by PKI. 8-Br-cAMP produced similar effect as $dmPGE_2$ which was blocked by co-treating with PKI. $^{a}P < 0.05$ vs. FSS + vehicle group, $^{b}P < 0.05$ vs. Pre-FSS group, $^{c}P < 0.05$ vs. FSS + $dmPGE_2$ group, $^{d}P < 0.05$ vs. FSS + 8-Br-cAMP group.

Quantification of the areal fractions of F-actin stress fibers

Under the present imaging and threshold settings, the areal fraction of continuous F-actin stress fiber in pre-FSS group was 0.28 ± 0.05, and was significantly increased to 0.79 ± 0.03 by FSS plus vehicle treatment. $dmPGE_2$ significantly suppressed the FSS-induced increment in F-actin stress fiber intensity (0.32 ± 0.05), which was comparable to the static level. Co-incubation of cells with phalloidin significantly attenuated the inhibition of $dmPGE_2$ (0.56 ± 0.03). Similarly, co-treatment with PKI significantly decreased the inhibition of $dmPGE_2$ (0.6 ± 0.03). The 8-Br-cAMP produced similar suppression as $dmPGE_2$ (0.45 ± 0.05) and was completely inhibited by PKI (0.78 ± 0.04) (**Fig. 2B,D**).

Downloaded from https://academic.oup.com/abbs/article/46/1/40/1399 by guest on 10 April 2024

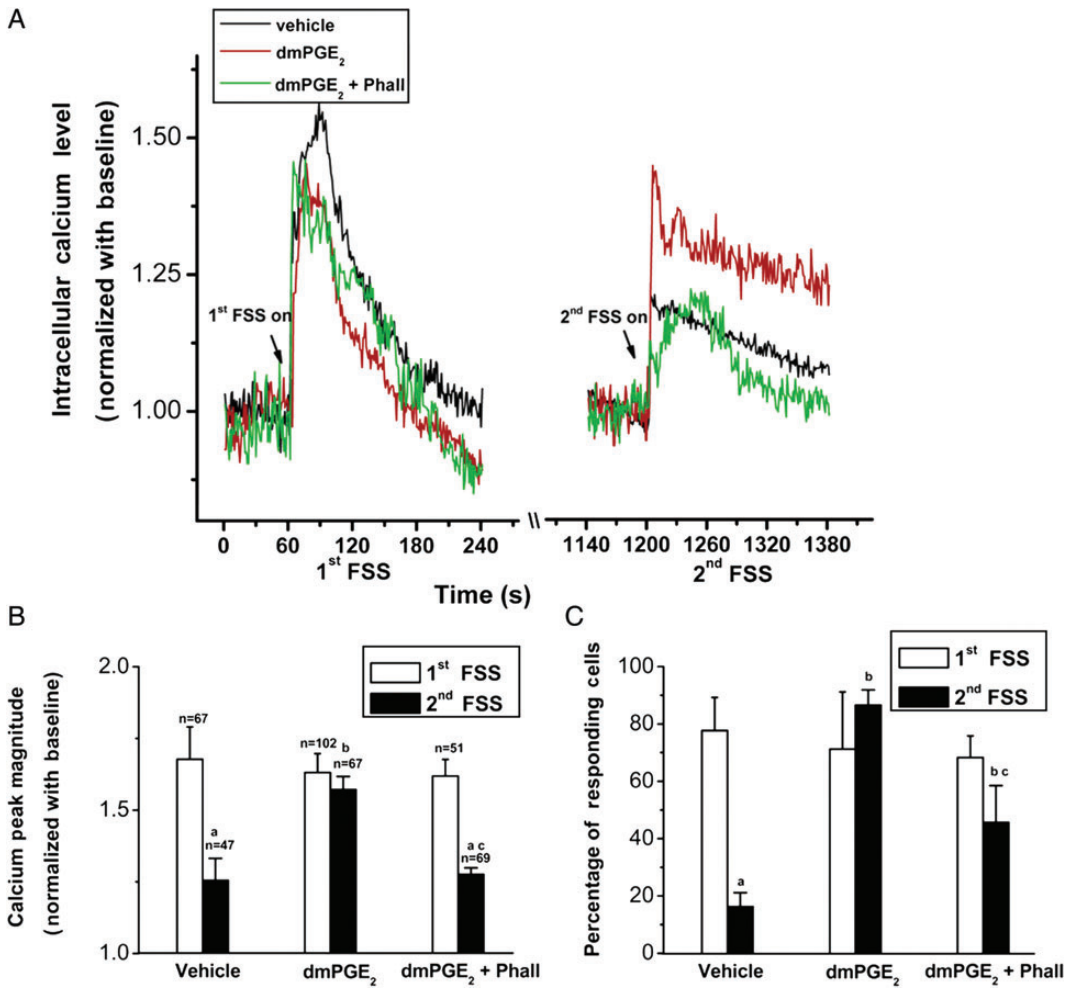

Figure 3. $dmPGE_2$ Modulates mechanosensitivity recovery (A) Representative traces of $[Ca^{2+}]_i$ responses during two bouts of FSS stimulation. (B) The calcium peak magnitude (baseline = 1) and (C) percentage of responding cells during two bouts of FSS stimulations. During the second FSS, the vehicle-treated cells showed reduced calcium peak-magnitude and the percentage of responding cells in the second FSS stimulation. In contrast, compared with first FSS, 10 nM PGE_2-treated cells showed no significant difference in calcium peak magnitude and an increased percentage of responding cells. Phalloidin (Phall) abolished the recovery of calcium peak magnitude and significantly attenuated the recovery of responding cells induced by $dmPGE_2$. Each experimental group was repeated thrice ($n = 3$ in C), 47–102 cells were used for data analysis (B). $^aP < 0.05$ vs. its own 1st FSS, $^bP < 0.05$ vs. second FSS in $dmPGE_2$ group, $^cP < 0.05$ vs. second FSS in vehicle group.

Effects of $dmPGE_2$ on the recovery of mechanosensitivity in MC3T3-E1 cells

Cells responded to the first FSS stimulation with a rapid increase in $[Ca^{2+}]_i$ in all groups (**Fig. 3**, first FSS). In detail, the average $[Ca^{2+}]_i$ peak magnitude and percentage of responding cells were 1.68 ± 0.11 and $77.7 \pm 11.6\%$ (52 of 67 cells) in the vehicle group, 1.63 ± 0.07 and $71.2 \pm 19.9\%$ (73 of 102 cells) in the $dmPGE_2$-treated group, and 1.62 ± 0.06 and $68.3 \pm 7.5\%$ (36 of 51 cells) in the $dmPGE_2$plus phalloidin group; no statistical difference was found among these groups. However, it was found that $dmPGE_2$ treatment, post the first FSS, significantly increased the cells' calcium peak magnitude and the percentage of responding cells in the second FSS stimulation by 1.25- and 5.31-fold, when compared with the vehicle treatment, which was respectively abolished and significantly attenuated by co-treating with phalloidin (**Fig. 3**, 2nd FSS). In detail, the average calcium peak magnitude and percentage of responding cells were 1.26 ± 0.08 and $16.3 \pm 4.8\%$ (8 of 47 cells) in the vehicle group, 1.57 ± 0.37 and $86.5 \pm 9.3\%$ (58 of 67 cells) in the $dmPGE_2$-treated group, and 1.28 ± 0.02 and $45.7 \pm 12.9\%$ (32 of 69 cells) in the $dmPGE_2$ plus phalloidin group.

Discussion

Mechanical forces and the downstream biochemical factors are important regulators for the maintenance of skeletal structure and mass. Osteoblasts respond to FSS with a $[Ca^{2+}]_i$ transient and a quick burst of ATP release (between 1–5 min post FSS), followed by a delayed, but sustained, PGE_2 release [8]. Previous studies have demonstrated a significant role of PGE_2 in osteoblasts' differentiation and proliferation [3–6]. The results from this study suggest a novel biological significance

Downloaded from https://academic.oup.com/abbs/article/46/1/40/1399 by guest on 10 April 2024

of PGE_2, which might counteract with early released adaptation-promoting factors, such as ATP. The initially released ATP has been shown to stiffen cells by increasing the polymerization of actin filaments, and thus, promote the adaptation of osteoblasts to their mechanical environment [8]. However, this increased cellular stiffness also caused the loss of mechanosensitivity by decreasing the FSS-induced cellular deformation and opening the possibility of iron channels [14,25]. One major effect of exogenous PGE_2, as derived from this study, is the resultant restoration of mechanosensitivity in osteoblasts, by way of softening cells through modulating F-actin stress fiber intensity post FSS stimulation. However, without the additional exogenous PGE_2, the effect of released ATP overrode the effect of PGE_2 on F-actin stress fiber due to the insufficient endogenous PGE_2 release (around 10^{-10}–10^{-9} M, induced by 20 min of 30 dyn/cm^2 FSS loading in MC3T3-E1 cells) [26], which was evidenced by fact that actin polymerization was still observed in vehicle group (**Fig. 2A**, b).

A reciprocal regulation mechanism existed between FSS-induced $[Ca^{2+}]_i$ transient and cytoskeleton remodeling. On one hand, as the earliest respondent upon receiving mechanical loading, $[Ca^{2+}]_i$ transient was thought to be responsible for the subsequent release of ATP and PGE_2, an alteration in gene expression [27] and cytoskeleton remodeling [28] in osteoblasts due to Ca^{2+} influx through the MSCC and voltage-sensitive Ca^{2+} channels (L-VSCC), as well as the intracellular Ca^{2+} release from endoplasmic reticulum [29]. On the other hand, treatments of cytochalasin D or parathyroid hormone disrupted/decreased F-actin stress fiber [14] increased the calcium response induced by FSS by decreasing the cellular stiffness, and modulating the open possibility of MSCC. Both sides suggested a direct connection between F-actin stress fiber and FSS-induced calcium response. In our study, we found that $dmPGE_2$ treatment increased the $[Ca^{2+}]_i$ transient during sequential FSS loading, which was abolished or attenuated by phalloidin. Our imaging quantification results showed that $dmPGE_2$ decreased the F-actin stress fiber intensity, while vehicle treatment increased it. These data together showed the participation of F-actin stress fiber in $dmPGE_2$ regulated mechanosensitivity in FSS-stimulated MC3T3-E1 cells. In addition, some cells in $dmPGE_2$ and phalloidin co-treated group showed delayed calcium peak (**Fig. 3A**, 2nd FSS), which suggested that phalloidin treatment caused the alteration of F-actin dynamics which might also be involved in mechanosensitivity in MC3T3-E1 cells.

Based on the observations that c-AMP/PKI respectively mimicked/attenuated the effect of PGE_2 on F-actin remodeling, we conclude that the PKA pathway is involved in PGE_2-induced F-actin remodeling. PGE_2 acts on osteoblasts through E-prostanoid (EP) receptors, in which EP1, EP2, and EP4 receptors are expressed in MC3T3-E1 cells [30]. EP2 and EP4 receptors are linked to Gs alpha subunit (G_s) to increase intracellular c-AMP level and activate PKA pathway [31]. Our preliminary data showed that PKA activation was able to augment the hypotonic stress induced $[Ca^{2+}]_i$ transient in MC3T3-E1 cells (**Supplementary Fig. S2A,B**), suggesting a potential role of PKA in PGE_2 induced mechanosensitivity recovery in osteoblasts. We speculated that when osteoblasts are stimulated by FSS, the released and exogenous PGE_2 might act through either or both EP2 and EP4 to activate PKA pathway and thus down-regulate F-actin intensity, eventually leading to the recovery of $[Ca^{2+}]_i$ transient (**Fig. 4**). Combined with previous reports showing that PKA pathway is involved in low-dose PGE_2 induced cell differentiation in osteoblasts [3,4], our and others' data suggested that PGE_2 might facilitate osteoblats to sense the FSS stimulation, thus amplifying the anabolic effect of FSS by promoting osteogenic differentiation. Our data also suggested that other signaling pathways might synergistically work with the PKA pathway, since PKA inhibition did not entirely blocked the effect of $dmPGE_2$ and c-AMP treatment was found not as effective as $dmPGE_2$ treatment.

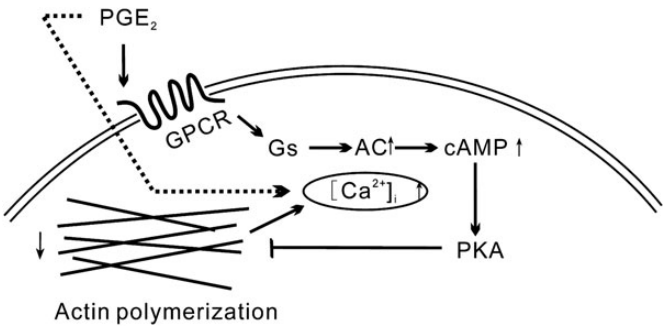

Figure 4. Proposed working model of extracellular PGE_2 on mechanosensitivity ($[Ca^{2+}]_i$) of FSS-stimulated MC3T3-E1 cells PGE_2 acted on EP receptor (GRCP), followed by release of Gs alpha subunit (Gs), cAMP elevation [as a consequence of the activation of adenylate cyclase (AC)], and PKA activation. The activated PKA pathway might suppress F-actin polymerization and cause the recovery of calcium response. Dash line indicates transmembrane; solid line, intramembrane.

In this study, a novel quantification method was used to measure the difference among different treatment groups in F-actin stress fiber. This quantification method has several strengths. First, the fluorescent intensity fluctuation among different batches of tests was unavoidable and exhibited a great impact on the accuracy of quantification results. We thus obtained a correction factor based on the nuclei staining intensity to limit the influence. Second, FSS-induced actin polymerization increased F-actin stress fiber thickness and length [8], causing an elongated cell morphology [32]. By using double thresholds defining system in our method, we were able to detect the area fraction of continuous F-actin stress fiber changes cell by cell between different treatment groups, which provided a better description about the F-actin stress fiber intensity than the total intensity ratio

Downloaded from https://academic.oup.com/abbs/article/46/1/40/1399 by guest on 10 April 2024

measurement used in previous studies [9,10]. However, there is still limitation in our study. The subtype(s) of EP receptor involved in $dmPGE_2$-modulated F-actin remodeling was not clear, since both EP2 and EP4 subtypes have been found to activate PKA pathway in different cell types [31,33,34]. In addition, to better describe the mechanism of PGE_2 modulated mechanosensitivity recovery, the involvement of the PKA pathway in PGE_2 modulated calcium response and RhoA activation, as well as the long-term effects of PGE_2 on mechanical loaded cells, needs to be further studied.

In conclusion, our study demonstrated that 10 nM $dmPGE_2$ was able to accelerate the 'reset' process of F-actin stress fiber to its pre-stimulated level partially through PKA pathway, thus promoting the recovery of cellular mechanosensitivity. Our finding provided a cellular mechanism by which PGE_2 increased bone formation *in vivo*, suggesting that PGE_2 could be a potential target for treatments of bone formation related diseases.

Supplementary Data

Supplementary data is available at *ABBS* online.

Funding

This work was supported by grants from the NIH (AR054385 and P20RR016458, DK058246, and AR051901), the National Natural Science Foundation of China (11272366, 11172207, and 10972243), the Visiting Scholar Foundation of Key Laboratory of Biorheological Science and Technology of Chongqing University, the Ministry of Education (No. CQKLBST-2012-002).

References

1. Gao Q, Xu M, Alander CB, Choudhary S, Pilbeam CC and Raisz LG. Effects of prostaglandin E2 on bone in mice *in vivo*. Prostaglandins Other Lipid Mediat 2009, 89: 20–25.
2. Tian XY, Zhang Q, Zhao R, Setterberg RB, Zeng QQ, Iturria SJ and Ma YF, *et al*. Continuous PGE2 leads to net bone loss while intermittent PGE2 leads to net bone gain in lumbar vertebral bodies of adult female rats. Bone 2008, 42: 914–920.
3. Hakeda Y, Yoshino T, Natakani Y, Kurihara N, Maeda N and Kumegawa M. Prostaglandin E2 stimulates DNA synthesis by a cyclic AMP-independent pathway in osteoblastic clone MC3T3-E1 cells. J Cell Physiol 1986, 128: 155–161.
4. Hakeda Y, Nakatani Y, Yoshino T, Kurihara N, Fujita K, Maeda N and Kumegawa M. Effect of forskolin on collagen production in clonal osteoblastic MC3T3-E1 cells. J Biochem 1987, 101: 1463–1469.
5. Hakeda Y, Hotta T, Kurihara N, Ikeda E, Maeda N, Yagyu Y and Kumegawa M. Prostaglandin E1 and F2 alpha stimulate differentiation and proliferation, respectively, of clonal osteoblastic MC3T3-E1 cells by different second messengers *in vitro*. Endocrinology 1987, 121: 1966–1974.
6. Miya T, Tagawa M, Kato N, Takahashi K, Sato K and Fujimura S. Involvement of protein kinase C in proliferative response of osteoblastic cell lines stimulated with prostaglandin E2. Biochem Mol Biol Int 1993, 29: 1023–1028.
7. McAllister TN and Frangos JA. Steady and transient fluid shear stress stimulate NO release in osteoblasts through distinct biochemical pathways. J Bone Miner Res 1999, 14: 930–936.
8. Gardinier JD, Majumdar S, Duncan RL and Wang L. Cyclic hydraulic pressure and fluid flow differentially modulate cytoskeleton re-organization in MC3T3 osteoblasts. Cell Mol Bioeng 2009, 2: 133–143.
9. Thi MM, Suadicani SO and Spray DC. Fluid flow-induced soluble vascular endothelial growth factor isoforms regulate actin adaptation in osteoblasts. J Biol Chem 2010, 285: 30931–30941.
10. Liu X, Zhang X and Lee I. A quantitative study on morphological responses of osteoblastic cells to fluid shear stress. Acta Biochim Biophys Sin 2010, 42: 195–201.
11. Cooper DE, Arnoczky SP and Warren RF. Arthroscopic meniscal repair. Clin Sports Med 1990, 9: 589–607.
12. Chen NX, Ryder KD, Pavalko FM, Turner CH, Burr DB, Qiu J and Duncan RL. Ca(2+) regulates fluid shear-induced cytoskeletal reorganization and gene expression in osteoblasts. Am J Physiol Cell Physiol 2000, 278: C989–C997.
13. Batra NN, Li YJ, Yellowley CE, You L, Malone AM, Kim CH and Jacobs CR. Effects of short-term recovery periods on fluid-induced signaling in osteoblastic cells. J Biomech 2005, 38: 1909–1917.
14. Zhang J, Ryder KD, Bethel JA, Ramirez R and Duncan RL. PTH-induced actin depolymerization increases mechanosensitive channel activity to enhance mechanically stimulated Ca2+ signaling in osteoblasts. J Bone Miner Res 2006, 21: 1729–1737.
15. Myers KA, Rattner JB, Shrive NG and Hart DA. Osteoblast-like cells and fluid flow: cytoskeleton-dependent shear sensitivity. Biochem Biophys Res Commun 2007, 364: 214–219.
16. Yang RS, Fu WM, Wang SM, Lu KS, Liu TK and Lin-Shiau SY. Morphological changes induced by prostaglandin E in cultured rat osteoblasts. Bone 1998, 22: 629–636.
17. Liu J, Chen L, Tao X and Tang K. Phosphoinositide 3-kinase/Akt signaling is essential for prostaglandin E2-induced osteogenic differentiation of rat tendon stem cells. Biochem Biophys Res Commun 2013, 435: 514–519.
18. Ryder KD and Duncan RL. Parathyroid hormone enhances fluid shear-induced [Ca2+]i signaling in osteoblastic cells through activation of mechanosensitive and voltage-sensitive Ca2+ channels. J Bone Miner Res 2001, 16: 240–248.
19. Jessop HL, Sjoberg M, Cheng MZ, Zaman G, Wheeler-Jones CP and Lanyon LE. Mechanical strain and estrogen activate estrogen receptor alpha in bone cells. J Bone Miner Res 2001, 16: 1045–1055.
20. Wadhwa S, Choudhary S, Voznesensky M, Epstein M, Raisz L and Pilbeam C. Fluid flow induces COX-2 expression in MC3T3-E1 osteoblasts via a PKA signaling pathway. Biochem Biophys Res Commun 2002, 297: 46–51.
21. Oishi A, Makita N, Sato J and Iiri T. Regulation of RhoA signaling by the cAMP-dependent phosphorylation of RhoGDIalpha. J Biol Chem 2012, 287: 38705–38715.
22. Regan JW, Bailey TJ, Pepperl DJ, Pierce KL, Bogardus AM, Donello JE and Fairbairn CE, *et al*. Cloning of a novel human prostaglandin receptor with characteristics of the pharmacologically defined EP2 subtype. Mol Pharmacol 1994, 46: 213–220.
23. Duncan RL, Hruska KA and Misler S. Parathyroid hormone activation of stretch-activated cation channels in osteosarcoma cells (UMR-106.01). FEBS Lett 1992, 307: 219–223.
24. Pan J, Zhang T, Mi L, Zhang B, Wang B, Yang L and Deng L, *et al*. Stepwise increasing and decreasing fluid shear stresses differentially regulate the functions of osteoblasts. Cell Mol Bioeng 2010, 3: 376–386.
25. Bacabac RG, Mizuno D, Schmidt CF, MacKintosh FC, Van Loon JJ, Klein-Nulend J and Smit TH. Round versus flat: bone cell morphology, elasticity, and mechanosensing. J Biomech 2008, 41: 1590–1598.

Downloaded from https://academic.oup.com/abbs/article/46/1/40/1399 by guest on 10 April 2024

26. Smalt R, Mitchell FT, Howard RL and Chambers TJ. Induction of NO and prostaglandin E2 in osteoblasts by wall-shear stress but not mechanical strain. Am J Physiol 1997, 273: E751–E758.
27. Genetos DC, Geist DJ, Liu D, Donahue HJ and Duncan RL. Fluid shear-induced ATP secretion mediates prostaglandin release in MC3T3-E1 osteoblasts. J Bone Miner Res 2005, 20: 41–49.
28. McGarry JG, Klein-Nulend J and Prendergast PJ. The effect of cytoskeletal disruption on pulsatile fluid flow-induced nitric oxide and prostaglandin E2 release in osteocytes and osteoblasts. Biochem Biophys Res Commun 2005, 330: 341–348.
29. Duncan RL, Akanbi KA and Farach-Carson MC. Calcium signals and calcium channels in osteoblastic cells. Semin Nephrol 1998, 18: 178–190.
30. Suda M, Tanaka K, Sakuma Y, Yasoda A, Ozasa A, Fukata J and Tanaka I, *et al*. Prostaglandin E(2) (PGE(2)) induces the c-fos and c-jun expressions via the EP(1) subtype of PGE receptor in mouse osteoblastic MC3T3-E1 cells. Calcif Tissue Int 2000, 66: 217–223.
31. Katsuyama M, Nishigaki N, Sugimoto Y, Morimoto K, Negishi M, Narumiya S and Ichikawa A. The mouse prostaglandin E receptor EP2 subtype: cloning, expression, and northern blot analysis. FEBS Lett 1995, 372: 151–156.
32. Kemeny SF, Figueroa DS and Clyne AM. Hypo- and hyperglycemia impair endothelial cell actin alignment and nitric oxide synthase activation in response to shear stress. PloS One 2013, 8: e66176.
33. Nishigaki N, Negishi M, Honda A, Sugimoto Y, Namba T, Narumiya S and Ichikawa A. Identification of prostaglandin E receptor 'EP2' cloned from mastocytoma cells EP4 subtype. FEBS Lett 1995, 364: 339–341.
34. Ohnishi A, Shimamoto C, Katsu K, Ito S, Imai Y and Nakahari T. EP1 And EP4 receptors mediate exocytosis evoked by prostaglandin E(2) in guinea-pig antral mucous cells. Exp Physiol 2001, 86: 451–460.

Downloaded from https://academic.oup.com/abbs/article/46/1/40/1399 by guest on 10 April 2024